JVSTB Journal of Vacuum Science & Technology B

Alkali antimonides photocathodes growth using pure metals evaporation from effusion cells

Luca Cultrera, Hyeri Lee, and Ivan Bazarov

Citation: Journal of Vacuum Science & Technology B **34**, 011202 (2016); doi: 10.1116/1.4936845
View online: http://dx.doi.org/10.1116/1.4936845
View Table of Contents: http://scitation.aip.org/content/avs/journal/jvstb/34/1?ver=pdfcov
Published by the AVS: Science & Technology of Materials, Interfaces, and Processing

Alkali antimonides photocathodes growth using pure metals evaporation from effusion cells

Luca Cultrera,[a] Hyeri Lee, and Ivan Bazarov
Cornell Laboratory for Accelerator Based Science and Education, Cornell University, Ithaca, New York 14853

(Received 4 September 2015; accepted 10 November 2015; published 2 December 2015)

The authors report on the growth of Na_2KSb bialkali and Na_2KSb:Cs_3Sb multialkali photocathodes using the vapors generated by evaporating pure metals with effusion cells under vacuum conditions. Details about the ultrahigh vacuum growth system and the used procedures are provided. The new growth system is capable of growing over large areas with uniform photoemission properties using different types of substrates. The measured spectral response curves indicate that high quality photocathodes are produced with peak quantum efficiencies well above 20%. Procedures to obtain multialkali photocathodes with extended sensitivity into the infrared range (well above 800 nm) are described. © *2015 American Vacuum Society*. [http://dx.doi.org/10.1116/1.4936845]

I. INTRODUCTION

Alkali antimonides semiconducting materials are of great interest for their use in photomultiplier (PMT) devices dedicated to single photon detection[1] and as electron sources for the generation of high brightness electron beams for next generation light sources like energy recovery linacs and free electron lasers.[2] Recent results also indicate that when operated near the photoemission threshold and at cryogenic temperature, these materials can generate electron beams with very low mean transverse energies equivalent to sub-room temperatures and due to their still relatively high quantum efficiency (QE) are viable candidates as electron sources for ultrafast electron diffraction experiment.[3]

Methods to synthesize alkali antimonides usually rely on the spontaneous chemical reaction of an Sb thin film with alkali metal vapors carried under ultrahigh vacuum conditions on a suitable substrate.[4] The photocurrent extracted from the alkali antimonide is commonly used as feedback during the synthesis to optimize growth conditions through maximizing the QE. Recently, attempts to synthesize alkali antimonides by UHV sputtering of a stoichiometric target have shown promising results as well.[5] Peak QE is one of the most important photocathode characteristic for single photon detection applications such as in high energy physics experiments where thousands of PMT are used in arrays to detect Cherenkov radiation generated by neutrinos decaying in large-scale water detector.[1] Alkali antimonide photocathodes are also used as electron sources for accelerator applications: here other parameters such as intrinsic emittance, response time, and operational lifetime become increasingly relevant.[2] When used as electron beam sources, the intrinsic emittance growth due to the roughness of the photocathode surface is another important parameter that needs to be minimized to be able to operate these materials under very high electric gradients typical of photoemission guns. Dedicated growth experiments to study the dynamics of the formation of these materials in real time using *in situ* x-ray diffraction techniques have been recently performed aiming at obtaining the smoother photocathode surfaces.[6] Nevertheless, the multiple requirements that will optimize the electron beam properties (high quantum efficiency, low intrinsic emittance, short response time, and long lifetime) cannot be satisfied by any known photocathode materials simultaneously as several of these parameters have conflicting dependences, and a trade-off is usually necessary to determine the best operating conditions depending on the specific use of the electron beam.[7]

During the growth of these materials, the Sb is commonly provided from high purity metallic beads via thermal evaporation. Alkali metal vapors can be obtained using different sources, including alkali metal chromates dispenser,[8] bismuth based alloys,[9–11] alkali azides,[12,13] and by evaporation of pure alkali metals.[14] The use of alkali chromates is advantageous because of their stability with respect to the exposure to open air and their compatibility with UHV environment, whereas alkali azides are also stable in open air, but they release large quantities of nitrogen gas upon decomposition that must be pumped away from the vacuum chamber. Bismuth based alloys and pure alkali metals are extremely reactive and their handling must occur in a glove box in the presence of an inert gas. Because of the drawbacks imposed by the handling of pure metals, only a handful of experiments have been performed to study the growth of alkali antimonide using pure alkalis as precursors demonstrating that photocathodes with QE comparable to the one reported for commercial devices can be achieved.[15–17]

The aim of this study is to explore the use of effusion cells loaded with pure metals in a geometrical configuration similar to the one adopted in molecular beam reactors for the growth of alkali antimonide based photocathode. First, we will detail the growth chamber that has been designed and built for this purpose. The design was chosen to be similar to that of the commercial molecular beam epitaxy reactors so that a simple scaling of the chamber should allow growth over larger area substrates suitable for present experiments like the large area photodetectors proposed by the LAPPD collaboration.[18] Finally, we will detail the recipe used for

[a]Electronic mail: lc572@cornell.edu

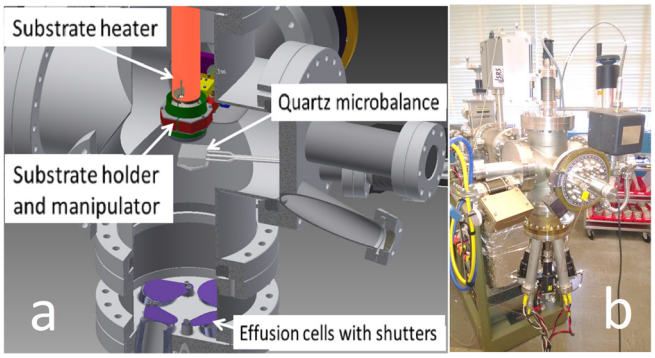

FIG. 1. (Color online) Three-dimensional model (a) and a picture (b) of the UHV growth chamber with effusion cells for evaporation of pure metals.

growth of high QE biantimonide photocathodes of the Na_2KSb type and the procedure we used to extend their sensitivity to longer wavelength by evaporating small additional amounts of Sb and Cs.

II. EXPERIMENTAL SETUP

The experimental setup for the growth of alkali antimonides family photocathodes consists of an UHV vacuum chamber as shown in Fig. 1. It is kept under vacuum by means of a 500 l/s ion pump. The alkali sources assembly is based on an 8 in. diameter ConFlat flange hosting four effusion cells (Varian Mod. 981-4134), each one equipped with its own pneumatically operated shutter. Because of the low melting point of alkali metals, the effusion cells have to be arranged so that the pyrolytic boron nitride (PBN) crucibles sit in an almost vertical position in order to prevent the spill of liquefied alkali metals into the chamber. The angle between the axis of the chamber and the axis of each furnace was chosen to be about 12°. With this geometrical configuration and the 5° of tapering angle characteristic of the PBN crucibles, the system provides a uniform overlap of the molecular fluxes within a 3 in. diameter circular area at about 20 cm distance from the top of the effusion cells.

In order to ensure compatibility with our other existing experimental vacuum chambers and with the Cornell high voltage DC guns,[19,20] a special substrate holder manipulator has been designed (Fig. 2). This manipulator is hosted by a differentially pumped rotatory platform so that a 90° rotation around the axis can be performed. This rotation gets the substrate holder from the loading/unloading position to the growth position, where the substrate must face the molecular fluxes generated by the effusion cells.

A resistive heater element is inserted from the top flange into the substrate holder and irradiation is used to heat the substrate up to about 600 °C. Two K type thermocouples are connected to the manipulator, and their reading is calibrated to monitor the substrate temperature.

The holder includes several ceramic insulators providing electrical insulation from the UHV chamber so that the substrate can be negatively biased to measure the photocurrent generated from the photocathode materials. In order to minimize the contribution to the photocurrent from stray light getting into the chamber, the light of laser diodes is modulated with a mechanical chopper, and the relative photocurrent is measured using a lock-in amplifier. The QE deduced from the measured photocurrent represents the main signal used as feedback during the synthesis of alkali antimonides photosensitive materials.

A water-cooled quartz crystal microbalance monitors the fluxes from the effusion cells. The microbalance is connected to a linear UHV translator allowing the crystal sensor to be moved just below the substrate surface or at about 2 in. distance from the center of the substrate. Measuring the ratio of the molecular fluxes between the two positions, when the cell is evaporating at a constant temperature, allows determining the tooling factor for each furnace. The tooling factor is then used to scale the quartz microbalance reading during the growth of photocathodes when the crystal sensor is moved away from the substrate.

Because of the high vapor pressure of alkali metals even at room temperature, a bake out of the growth chamber cannot be performed once the effusion cells have been loaded with alkali metals. For this reason, the chamber is baked before loading the metals into each crucible, and the effusion cells and crucibles are degassed by raising their temperature up to 400 °C. After the bake, the chamber is vented with a high purity argon gas. A glove bag is connected to the source flange and purged with argon gas for a few hours. The effusion cells are then removed one by one, and the crucibles are filled with the alkali metals inside the glove bag without exposing them to air. Once all the cells have been refilled

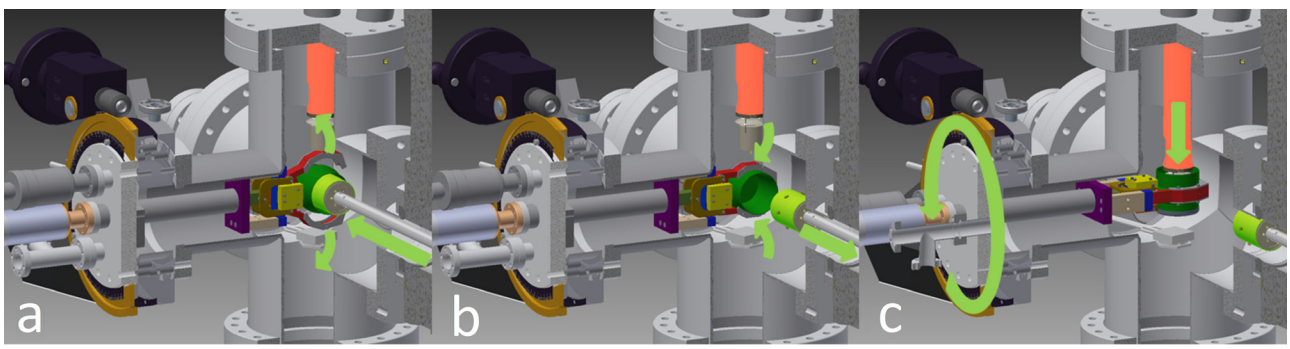

FIG. 2. (Color online) Manipulator and rotary platform operation, which allows the substrate holder to be loaded (a), released (b), and rotated (c) to face the effusion cells hosted in the bottom flange. A resistive heater element is inserted from the top (shown on the right).

and reconnected, the growth chamber is pumped down to UHV. Effusion cells' crucibles are filled with 5 g of Cs, K, Na, and Sb each. After 24 h of pumping, the vacuum level reached a typical level of few 10^{-8} Torr. Refer to Fig. 3 for the mass spectrum as measured with a residual gas analyzer (SRS RGA-200).

The mass spectrum in Fig. 3 is hydrogen dominated along with water vapors in the low 10^{-10} Torr range. It is important for water vapors to be kept as low as possible to avoid poisoning of the photocathode during and after the growth. Assuming a sticking coefficient equal to one, the time for the formation of a single monolayer of water vapor is estimated to be about 3 h. From the mass spectrum, we can also see that Cs vapors are already detected even with the effusion cell kept at room temperature; the measured partial pressure for singly ionized Cs ions is in the 10^{-11} Torr range (which is equivalent to a time span of few hours for the formation of a single monolayer over the photocathode surface).

III. RESULTS AND DISCUSSION

Photocathode growth experiments were performed on polished 304 stainless steel substrates and on Borofloat 33 glass. The stainless steel substrates were optically polished by using colloidal diamond suspensions with decreasing particulate sizes (from 15 μm to 100 nm). Figure 4 reports a typical surface morphology of the stainless steel substrate after the polishing as obtained using an optical interferometric profiler (ADE Phase Shift MicroXAM). The RMS roughness is determined to be about 3 nm.

The 2.5 mm thick Borofloat 33 glass substrates were simply rinsed in isopropyl alcohol then loaded into a dedicated hollow substrate holder, which allows illuminating the photocathode in transmission mode through the back of the substrate. The electrical contact between the photocathode film and the substrate holder is ensured by a 30 μm thick indium metal foil, which is used to solder the retaining mask with the four corners of the glass substrate, as shown in Fig. 5.

Once the substrate has been loaded into the growth chamber, the heater is inserted into the back of the holder (as shown in Figs. 1 and 2) and turned on to raise the substrate temperature to 550 °C. During heating, puck and substrate are allowed to degas for at least 24 h until the vacuum

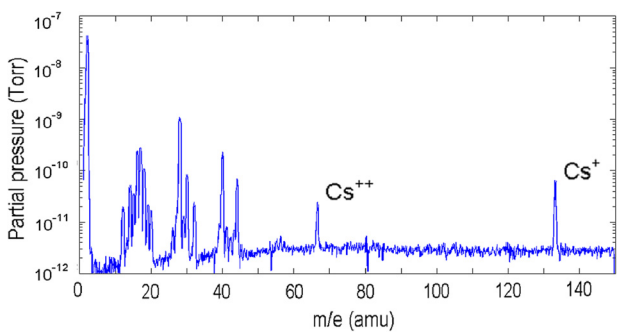

FIG. 3. (Color online) RGA mass spectrum: peaks of Cs single and doubled ionized are labeled.

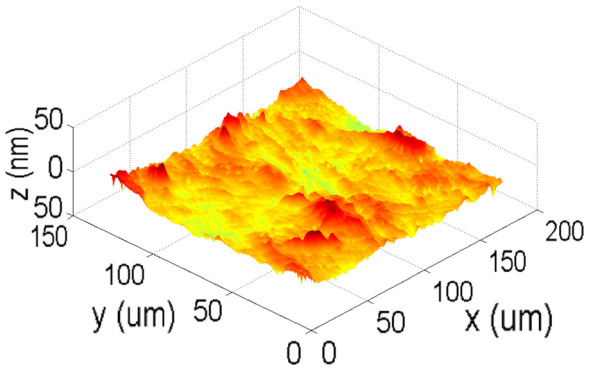

FIG. 4. (Color online) Typical surface morphology of polished stainless steel photocathode substrates.

pressure in the chamber recovers back to few 10^{-9} Torr. At this point, the substrate temperature is lowered to about 160 °C by decreasing the current through the resistive heater.

A typical growth of a Na_2KSb photocathode proceeds as follows (see Fig. 6). The Sb effusion cell temperature is raised to about 490 °C and a 20 nm thin layer of Sb is then deposited over the substrate surface with a quartz microbalance detected deposition rate of about 0.6 nm/min (Sb flux is 4×10^{13} atoms cm^{-2} s^{-1}). During the Sb deposition, the temperature of the effusion cell hosting the K is raised to 110 °C. When the growth of the Sb layer is completed, the Sb effusion cell shutter is closed, the temperature of the cell is decreased to 275 °C (preventing alkali metal deposition onto the Sb effusion cell surfaces), and the shutter of the K effusion cell is opened to allow exposure of Sb layer to K vapors (K flux is 3×10^{14} atoms cm^{-2} s^{-1}). At the same time, the substrate heater is turned off allowing the substrate to slowly cool down to room temperature by radiative losses. The photocurrent generated by illuminating with a laser light at 532 nm increases as K evaporation continues and is seen to peak when QE reaches about 1%. As the last step, the K effusion cell shutter is closed, and the shutter of the Na effusion cell is opened. The Na effusion cell is heated to 150 °C (Na flux is 3×10^{13} atoms cm^{-2} s^{-1}), and the photocurrent is seen to further increase up to a QE of about 5%.

After the growth, the spectral response of the photocathode is measured as function of the wavelength. A lamp

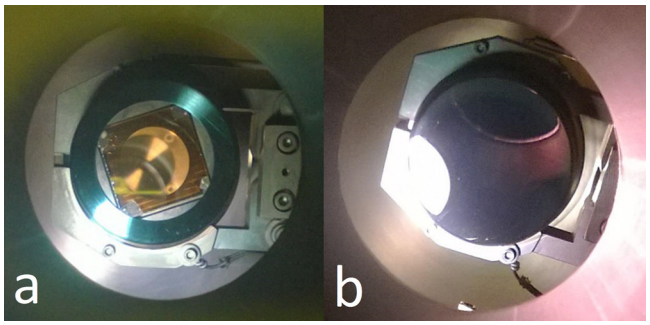

FIG. 5. (Color online) Pictures of different used substrate and holders: (a) square glass substrate held by a metallic retaining ring. Photocathode film is semitransparent. (b) Photocathodes are grown over the polished surface of stainless steel holder. Substrate mirror-like finish is preserved after the growth.

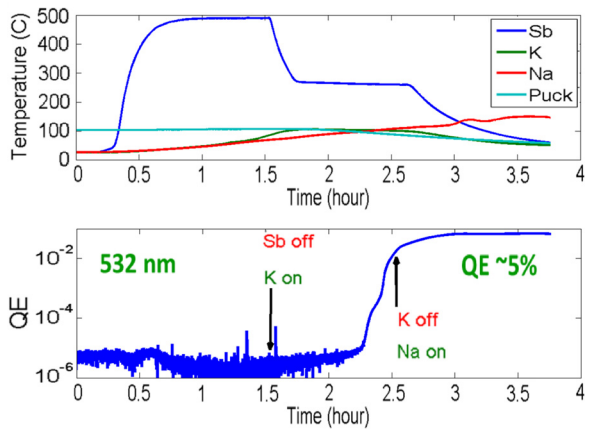

FIG. 6. (Color online) Na_2KSb growth history. Note that according to previous calibrations, the substrate temperature is about a factor 1.6 larger than the temperature measured at the thermocouple location.

and a monochromator provide the variable wavelength light in the range of 400–900 nm. A typical spectral response of a Na_2KSb photocathode grown with the above-described procedure is reported in Fig. 7. Quantum efficiencies larger than 20% are typically obtained at 400 nm.

All of the deposition experiments have been conducted without using any masks typically employed to limit the active area, so that photocathode materials were deposited over the entire available substrate surface. Figure 8 shows another picture of an actual photocathode grown over a stainless steel polished substrate having a diameter of about 45 mm (the color of the whole substrate area uniformly turned purple due to the presence of the thin alkali antimonide film without losing its mirror-like finish) and the QE scan of the central $15 \times 15\,mm^2$ area obtained by scanning the 532 nm laser over the surface, indicating a 10% uniformity of the emission within this area (the scan range was limited by our current setup).

To extend to the IR part of the spectrum, the otherwise limited sensitivity of Na_2KSb photocathodes (to less than

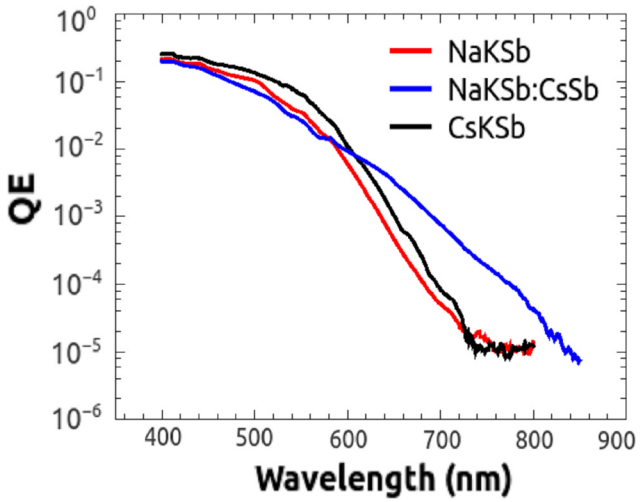

FIG. 7. (Color online) Spectral response for a reflection mode Na_2KSb photocathode grown over a polished stainless steel substrate. The CsK_2Sb data of the sample with the highest QE obtained in our previous growth system is shown for a comparison.

740 nm), we attempted to grow a very thin Cs_3Sb layer over the Na_2KSb surface. It is expected that due to the formation of a p-n junction at the interface between the intrinsic p-type Na_2KSb and the n-type Cs_3Sb, the photoexcited electrons lying near the bottom of the conduction band within the Na_2KSb layer can travel through the Cs_3Sb and be extracted to vacuum as described in Ref. 21. This mechanism has proven to enable photoemission in the infrared part of the spectrum. A correct dosing of Cs and Sb over the surface of the Na_2KSb photocathode results in an extended response of the photocathode in the infrared all the way to about 1 μm wavelength. To perform this growth, we used alternating evaporations of Sb and Cs over the surface of several Na_2KSb photocathodes, which were first allowed to cool down to room temperature.

The source flange was designed and built to include a mechanical shutter for each individual effusion cell used to evaporate Sb and alkali metals. This addition was made to improve the control and triggering of the vapors fluxes directed at the substrate. Unfortunately, despite some promising results, this initial design was not free of some drawbacks. Operating the shutters induced a nonnegligible change of the heat losses for each furnace so that temperature drifted by a 10–15 °C over few minutes when the shutters were activated (the opening and closing of the shutter produced a decrease and an increase of the cell temperature, respectively). Due to the absence of any feedback loop to control the cells temperatures by a proper tuning of the current through the heater element aimed at mitigating this effect, we increased the distance between the shutter and the top of the crucible to ~5 mm from the original ~1 mm design value. This increased distance helped in reducing the temperatures drifts to few degrees Celsius and increased the time constant of the variation to several tens of minutes, which allowed the experimenter to fine tune the electric power to compensate for the drift and to obtain a more accurate control of the evaporation rate. However, because of the larger gap, the shutter was unable to completely turn off the flux of the elements, especially in the case of Cs, which is the most volatile of the alkali species used in these experiments.

Another deficiency in the design of the source flange was the absence of any heat shield between the effusion cells, which also resulted in an unwanted temperature drift of all

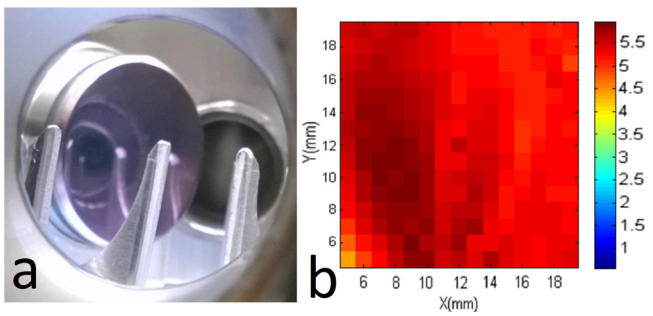

FIG. 8. (Color online) Photocathode thin film over the polished SS substrate (a) and a QE scan of the photocathode surface at 532 nm over a $15 \times 15\,mm^2$ area (b).

alkali metal furnaces (up to 15 °C) whenever the Sb effusion cell was heated to about 500 °C to perform the metal evaporation. A new flange to host the effusion cells has been designed aiming at mitigating the unwanted temperature drifts and to improve the shutter efficiency and is currently under assembly.

During the exposure of the Na_2KSb photocathodes to Cs and Sb vapors, the photocurrent was extracted from the photocathode surface while illuminating the front surface with a laser diode emitting at 780 nm.

At this wavelength, a typical Na_2KSb grown using the procedure detailed above has a QE below our detectable threshold (low 10^{-5}) as reported in the spectral response curve shown in Fig. 7. During the exposure of the Na_2KSb photocathodes to alternating Sb and Cs vapors, very small fluxes (on the range of few 10^{12} atoms cm^{-2} s^{-1}) have been used allowing a slow growth and hence a fine tuning of the Cs_3Sb thickness to maximize the QE.

The photocurrent extracted at 780 nm was then used as a feedback to trigger the fluxes on and off. Three Na_2KSb photocathodes have been exposed to Cs and Sb vapors (Fig. 9). The final QEs obtained at 780 nm with this procedure ranged between 3×10^{-5} and 5×10^{-4}. While these numbers are promising and show that we do extend the sensitivity of our photocathodes to the infrared part of the spectrum, the QEs measured at 780 nm so far were still an order of magnitude lower than those obtained in the photomultipliers tubes for similar materials.

The spectral response curve of one these photocathodes with a larger infrared sensitivity is reported in Fig. 7 (blue line) along with typical spectral response of Na_2KSb and CsK_2Sb photocathodes grown in our lab. The spectral response of the Na_2KSb:Cs_3Sb photocathodes is larger than that of other bialklai antimonide materials for wavelengths longer than 600 nm and photoemission is now detected even at wavelengths well beyond 800 nm.

Growth experiments were performed on glass substrates to realize semitransparent photocathode to be operated in a transmission mode (Fig. 5 shows one of these photocathodes). The procedure we followed to realize Na_2KSb photocathodes was the same one used to grow the reflecting mode photocathodes on stainless steel substrate, including the 20 nm thickness of the initial Sb layer. The spectral responses from this photocathode in the reflecting and the transmission modes are reported in Fig. 10.

The spectral response shows that when operated in the reflection mode, the Na_2KSb grown on glass has a typical QE of other samples grown on stainless steel substrates (a maximum measured QE of about 20% at 400 nm). On the other hand, when the photocathode is operated in the transmission mode, the measured QE is noticeably smaller. This is likely due to the not-yet-optimized thickness of the initial layer of Sb, which yields the final photosensitive film with a thickness much larger than the mean free path of electrons inside the alkali antimonide thin film. As a result, a good fraction of the excited electrons that are generated near the interface between the glass and alkali antimonide reach the vacuum barrier on the other side of the alkali antimonide film having lost too much energy and are unable to overcome the electron affinity barrier to escape into vacuum resulting in a smaller QE than the one obtained in the reflection mode. The maximum QE measured in the transmission mode for this sample grown on a glass substrate is slightly larger than 6% for a wavelength of 440 nm.

IV. SUMMARY AND CONCLUSIONS

We report on the growth of high QE photocathodes for use in photon detection or as photoelectron source for accelerator based next generation light sources. Growth experiments have been performed by evaporating pure metals from effusion cells. This growth method resulted in photocathodes with peak quantum efficiencies above 20% over the investigated spectral range (400–900 nm). Details on the growth chamber and of the used procedures are given. Growth experiments have been limited to samples with a diameter of about 2 in but a simple scaling of the growth chamber should allow uniform deposition over larger substrates for application in large area photodetectors. Multialkali photocathodes have been also synthesized showing sensitivity extending further in the

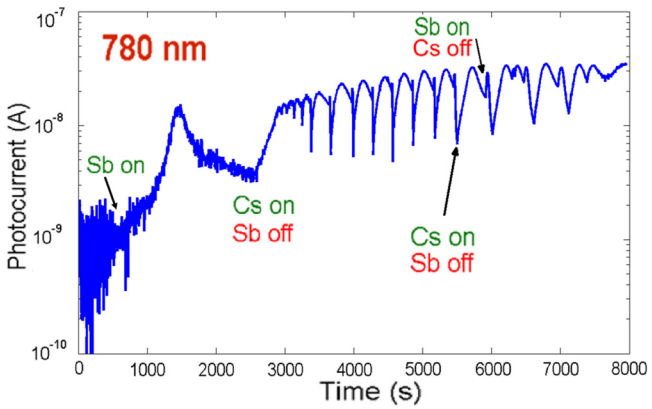

FIG. 9. (Color online) Photocurrent extracted from a Na_2KSb illuminated with light at 780 nm during exposure to alternating fluxes of Sb and Cs vapors.

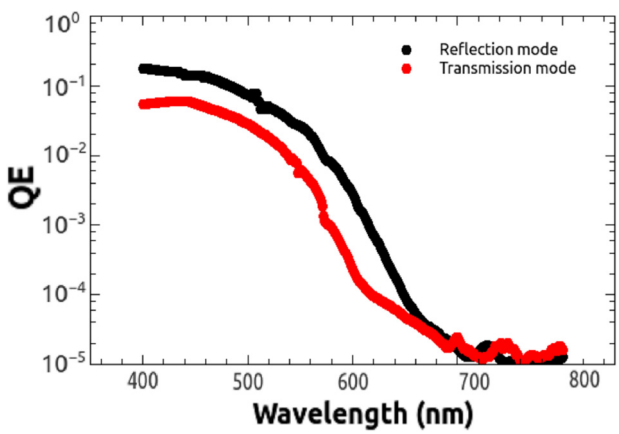

FIG. 10. (Color online) Spectral response of a Na_2KSb photocathode grown over a glass substrate when illuminated in reflection and transmission mode.

infrared part of the spectrum. Quantum efficiencies as large as 5×10^{-4} have been obtained at 780 nm.

ACKNOWLEDGMENTS

This work was supported by DOE under the Award No. DE-SC0011643 and by NSF under the Award No. PHY-1416318.

[1]M. Bergevin, AIP Conf. Proc. **1663**, 100002 (2015).
[2]D. H. Dowell *et al*., Nucl. Instrum. Methods A **622**, 685 (2010).
[3]L. Cultrera, S. Karkare, H. Lee, X. Liu, I. Bazarov, and B. Dunham, Phys. Rev. ST Accel. Beams **18**, 113401 (2015).
[4]M. Ruiz-Osés *et al*., APL Mater. **2**, 121101 (2014).
[5]J. Smedley *et al*., *Proceedings of the 6th International Particle Accelerator Conference*, Richmond, VA, USA, Paper No. TUPHA003 (2015), pp. 1965–1967.
[6]J. Smedley *et al*., *Proceedings of the 35th International Free-Electron Laser Conference*, New York, NY, USA, Paper No. TUPS076 (2013), pp. 403–405.
[7]J. Maxson, L. Cultrera, C. Gulliford, and I. Bazarov, Appl. Phys. Lett. **106**, 234102 (2015).
[8]"Alkali metals dispensers," https://www.saesgetters.com/products/alkali-metals-dispensers.
[9]J. Sangster and A. D. Pelton, J. Phase Equilib. **12**, 451 (1991).
[10]J. Sangster and A. D. Pelton, J. Phase Equilib. **12**, 443 (1991).
[11]A. Petric and A. D. Pelton, J. Phase Equilib. **12**, 29 (1991).
[12]F. Blatter and E. Schumacher, J. Less–Common Met. **115**, 307 (1986).
[13]L. Cultrera, M. Brown, S. Karkare, W. Schaff, I. Bazarov, and B. Dunham, J. Vac. Sci. Technol. **32**, 031211 (2014).
[14]M. A. Mamun, C. Hernandez-Garcia, M. Poelker, and A. A. Elmustafa, APL Mater. **3**, 066103 (2015).
[15]N. Massegu, A. Konrath, J. M. Barois, P. Christol, and E. Tournié, Electron. Lett. **44**, 315 (2008).
[16]I. A. Dubovoi, A. S. Chernikov, A. M. Prokhorov, M. Y. Schelev, and V. K. Ushakov, Proc. SPIE **1358**, 134 (1991).
[17]V. V. Balanyuk, A. S. Chernikov, V. F. Krasnov, S. L. Musher, V. E. Ryabchenko, A. M. Prokhorov, I. A. Dubovoi, V. K. Ushakov, and M. Y. Schelev, Proc. SPIE **945**, 68 (1988).
[18]M. J. Minot *et al*., Nucl. Instrum. Methods A **787**, 78 (2015).
[19]J. Maxson, I. Bazarov, B. Dunham, J. Dobbins, X. Liu, and K. Smolenski, Rev. Sci. Instrum. **85**, 093306 (2014).
[20]B. Dunham *et al*., Appl. Phys. Lett. **102**, 034105 (2013).
[21]A. Natarajan, A. T. Kalghatgi, B. M. Bhat, and M. Satyam, J. Appl. Phys. **90**, 6434 (2001).